# Contrast Gain Control in the Lower Vertebrate Retinas

HIROKO M. SAKAI,* J.-L. WANG,* and KEN-ICHI NAKA*,‡

From the *Department of Ophthalmology and ‡Department of Physiology and Biophysics, New York University Medical Center, New York, New York 10016

ABSTRACT Control of contrast sensitivity was studied in two kinds of retina, that of the channel catfish and that of the kissing gourami. The former preparation is dominantly monochromatic and the latter is bichromatic. Various stimuli were used, namely a large field of light, a spot-annulus configuration and two overlapping stimuli of red and green. Recordings were made from horizontal, amacrine, and ganglion cells and the results were analyzed by means of Wiener's theory, in which the kernels are the contrast (incremental) sensitivity. Modulation responses from horizontal cells are linear, in that the waveform and amplitude of the first-order kernels are independent of the depth of modulation. In the N (sustained) amacrine and ganglion cells, contrast sensitivity was low for a large modulation input and was high for a small modulation input, providing an example of contrast gain control. In most of the cells, the contrast gain control did not affect the dynamics of the response because the waveform of the first-order kernels remained unchanged when the contrast sensitivity increased more than fivefold. The signature of the second-order kernels also remained unchanged over a wide range of modulation. The increase in the contrast sensitivity for the second-order component, as defined by the amplitude of the kernels, was much larger than for the first-order component. This observation suggests that the contrast gain control proceeded the generation of the second-order nonlinearity. An analysis of a cascade of the Wiener type shows that the control of contrast sensitivity in the proximal retinal cells could be modeled by assuming the presence of a simple (static) saturation nonlinearity. Such a nonlinearity must exist somewhere between the horizontal cells and the amacrine cells.

The functional implications of the contrast gain control are as follows: (*a*) neurons in the proximal retina exhibit greater sensitivity to input of lower contrast; (*b*) saturation of a neuronal response can be prevented because of the lower sensitivity for an input with large contrast, and (*c*) over a large range of modulation depths, the amplitude of the response remains approximately constant.

## INTRODUCTION

Under natural conditions, visual input is a modulation of a steady mean luminance that changes very slowly. Such visual inputs come mostly from the reflecting surface.

Address correspondence to Ken Naka, NYU Medical Center, 550 First Avenue, PHL-821, New York, NY 10016.

J. GEN. PHYSIOL. © The Rockefeller University Press · 0022-1295/95/06/0815/21 $2.00
Volume 105 June 1995 815–835

Therefore, animals have evolved in a world of reflecting surfaces (Shapley, Kaplan, and Purpura, 1993). The relationship between the magnitude of modulation and the amplitude of the response is, therefore, one of the important measures of retinal function. In their series of experiments on ganglion cells of the cat retina, Shapley and Victor (1978, 1979, 1981) and Victor (1987, 1988) discovered that the sensitivity of a ganglion cell, measured as the number of spikes per second per unit contrast, was greater for an input with a smaller depth of modulation than for an input with a larger modulation. Shapley and Victor (1978, 1979, 1981) chose the term "contrast gain control," to describe this phenomenon. From the dependence on frequency of the gain curve, Shapley and Victor (1978, 1979, 1981) concluded that the gain control was not a simple response saturation but could be considered a frequency-dependent saturation. Shapley and Victor coined the phrase "an automatic control of contrast." Since Shapley and Victor's discovery, a number of papers have been published on this subject (Ohzawa and Freeman, 1985; Benardete, Kaplan, and Knight, 1991).

In this paper we present a phenomenological description of the dependence of sensitivity of retinal neurons on the depth of modulation in the retinas of two fish, the channel catfish and the kissing gourami. We shall define contrast sensitivity by the first-order and second-order kernels that include the response dynamics.

Five conclusions can be drawn from the present study: (*a*) The contrast sensitivity of a horizontal cell does not depend on the depth of input modulation. (*b*) The contrast sensitivity of neurons in the inner retina depends on the depth of modulation but response dynamics are independent of changes in contrast sensitivity. (*c*) Constancy of the response amplitude, the output, is maintained over a large range of modulation depths, the input. (*d*) The control or contrast gain that we observed can be modeled by a simple saturating nonlinearity. (*e*) Different neuronal mechanisms for control of contrast sensitivity exists in the retinas of higher and lower vertebrates.

## MATERIALS AND METHODS

Experiments were performed on eye-cup preparations of the channel catfish, *Ictalurus punctatus,* and the kissing gourami, *Helostoma temmincki.* Recordings were made intracellularly as well as extracellularly in the conventional manner. Data were first stored on digital audiotapes (DAT), with a data recorder (RD-101T; TEAC, Tokyo, Japan) and analyses were made off-line using a software system, STAR (Spatio-temporal Analysis Routines) developed by a team led by Dr. Masanori Sakuranaga (National Institute for Basic Biology, Okazaki, Japan). For white-noise analysis, data were digitized at a rate of 0.5 kHz and for waveform displays, they were digitized at a rate of 4 kHz. The software was run on a combination of μVAX3600 (Digital Equipment, Maynard, MA) and an AP-5000 array processor (Floating Point Systems, Portland, OR). White-noise signals were generated by a 1360 Burst Random Noise Generator (NF Electric Instruments, Tokyo, Japan).

Visual stimulation: a two-channel photo-stimulator was used to provide three types of stimuli: (*a*) a large field of red light covering the whole eye-cup preparation; (*b*) a spot and a concentric annulus of light both derived from a red LED; and (*c*) two overlapping large fields of red and green lights. We used a red and a green LED (H-3000 and HBG556X, Stanley, Tokyo). The first two types of stimulus configurations were used mainly in experiments with catfish and the third type in experiments with the kissing gourami. Parameters of stimulus configurations can be found in the legends to figures. We used spots of three diameters, 0.1, 1.2, and 2.5 mm and

annuli, with two inner diameters, 1.5 and 3.0 mm. The outer diameter of the annulus was 5.0 mm in every case. We chose the combination of a spot and an annulus that produced the optimal separation of the responses from a receptive field center and surround. Illuminance of the light stimulus was calibrated with a LI-19C quantum sensor (LI-Cor, Lincoln, NB). Unless otherwise indicated, the mean luminance was $1.9 \times 10^{11}$ photons/mm$^2$/s for the red input and $9 \times 10^{10}$ photons/mm$^2$/s for the green input.

Definition of terms: the mathematical definitions of terms used in this paper can be found in Sakuranaga and Naka (1985).

Cell type identification: in catfish we used the standard classification scheme that we have used in the past (Sakai and Naka, 1988). In the kissing gourami, injections of lucifer yellow or neuro-tracer were used to identify the morphological origin of a response. Classification was based on the large number of cells that have been identified functionally as well as morphologically since 1990 (Sakai, Machuca, and Naka, manuscript in preparation).

### *Definition of Sensitivity*

Illumination, $L(t)$, falling onto the retinal surface is generally presented as the sum of two terms, a steady mean illuminance, $I_0$, and an illuminance modulation, $i(t)$ which has an average value of zero:

$$L(t) = I_0 + I(t). \tag{1}$$

Within a second-order approximation, the response, with the exception of spike discharges, can be expressed as:

$$v(t) = \int_0^\infty h_1(\tau) i(t - \tau)\, d\tau + \int_0^\infty \int_0^\infty h_2(\tau_1, \tau_2) i(t - \tau_1) i(t - \tau_2)\, d\tau_1 d\tau_2. \tag{2}$$

We make the simplifying assumption that the modulation of the response is linearly related to the modulation of the input. When a brief test flash of intensity $I^*$ and duration $\Delta t$ is applied at $t = 0$ on a steady background $I_0$, the response can be written as:

$$V(t) = V_0(I_0) + I^* \Delta t \cdot h_1(\tau; I_0). \tag{3}$$

The incremental sensitivity, $S_i(t)$, of a cell is defined as the change $\Delta V(t)$ in the potential generated by a criterion stimulus of strength $\Delta I = I^* \Delta t$, as follows:

$$S_i(t) = (\Delta V(t))/\Delta I = h_1(\tau; I_0). \tag{4}$$

Thus, incremental sensitivity as defined here includes the cell's response dynamics and is generally a function of mean illuminance. In the past, the kernels were used to characterize the incremental sensitivity of retinal neurons in various animals, as follows: in catfish (Naka, Chan, and Yasui, 1979), in turtle (Chappell, Naka, and Sakuranaga, 1985; Naka, Itoh, and Chappell, 1987), in cockroach (Mizunami, Tateda, and Naka, 1986), and in skate (Naka, Chappell, Sakuranaga, and Ripps, 1988). The classical Weber-Fechner relationship represents the statics of the sensitivity and the kernel analysis added the response dynamics. Contrast sensitivity is a function of depth of modulation and, at one certain mean level, $I_0$, is related to incremental sensitivity, $I/\Delta I$, at that same level as follows:

$$S_c(t) = (\Delta V(t))/(\Delta I/I_0) = I_0 \cdot h_1(\tau; I_0) \tag{5}$$

When $I_0$ is kept at a steady level, $h_1(\tau;I_0)$ is the contrast sensitivity for an input $I(t)$. Similarly, the second-order kernel, $h_2(\tau_1,\tau_2;I_0)$, is the contrast sensitivity of the second-order component. Here we are looking for the relationships between the changes in $I(t)$ at a given $I_0$ and the resultant first-order, $h_1(\tau;I_0)$, and second-order kernels, $h_2(\tau_1,\tau_2;I_0)$. The principal reason why

kernels provide a measure of the sensitivity is that the kernels are scaled by the power, $P$, of the input. A more detailed description of Wiener kernels as a measure of sensitivity can be found in the work of Sakuranaga and Ando (1985). Contrast, namely, the depth of modulation, is defined by $(I_{max} - I_{min})/(I_{max} + I_{min})$ where, for white noise stimuli, $I_{max}$ and $I_{min}$ are three standard deviations greater and less than $I_0$, which is equal to $(I_{max} + I_{min})/(2L$ mean). This is an example of Rayleigh contrast (Shapley and Enroth-Cugell, 1984).

Probability density function, PDF, of $x$ is defined as:

$$p(x) = Nx/Ns\Delta x \tag{6}$$

where $N$ is the total number of data points sampled and $Nx$ is the number of data points falling within the narrow range, $x \pm \Delta x/2$, within an interval $\Delta x$. In a linear system, a Gaussian input produces an output PDF of Gaussian distribution. The skewness appearing in a PDF is a simple measure of nonlinearity: conversely, if the PDF of a response evoked by a Gaussian input is Gaussian, the response is possibly linear (McKean, 1973). The linearity can be confirmed in a quantitative fashion by the mean square error, MSE (Sakuranaga and Naka, 1985). Most of PDFs shown in this paper are fitted with the best fitting Gaussian function.

In this paper we will show diagonal cuts of the second-order kernels to facilitate the comparison of several kernels generated by stimuli of different depths of modulation. The cut is made through a plane in which $\tau_1 = \tau_2$.

### *Spike Discharges*

Spike discharges were transformed into unitary pulses of 2 ms in duration and kernels were computed using the same algorithms as were used for the analogue response. This approach is based on our heuristic finding that the generation of spike discharges is nonlinear but is approximately static (Korenberg, Sakai, and Naka, 1989). Generation of spike discharges can be approximated by a cascade of the Wiener type in which a linear dynamic filter is followed by a high-order but static nonlinearity. The process of cross-correlation makes the high-order nonlinearity transparent, in other words, it appears as if the nonlinearity has been removed (Korenberg, 1973). In the past we have shown that cross-correlation between the light input and the ganglion cell's postsynaptic potential and spike discharges generated two sets of first- and second-order kernels which were similar in their waveforms for both catfish and frog retinas (Sakuranaga, Ando, and Naka, 1987). Interpretation of the spike kernels is, therefore, identical to that of the analogue potentials. The first-order (spike) kernels are also identical in their waveform to those computed by the reverse correlation but time runs in the opposite direction (deBoer and Kuyper, 1968; Meister, Pine, and Baylor, 1993).

## RESULTS

### *Horizontal Cells*

Fig. 1 *A* shows a series of modulation responses from luminosity horizontal cells of the kissing gourami that were evoked by a large field of red light. A steady illuminance, $I_0$, (Fig. 1 *A1*), produced a steady hyperpolarization, $V_0$, of 15 mV, (Fig. 1 *A2*). In general, the relationship between $I_0$ and $V_0$ resembles the Michaelis-Menten equation (Naka and Rushton, 1967) and it defines the absolute (DC) sensitivity (Naka et al., 1979). As in the case of the turtle horizontal cells (Chappell et al., 1985), the peak value of a response, $V_p$, (Fig. 1 *B2*), evoked by a pulsatile input with an amplitude $I_0$ (Fig. 1 *B1*), is not identical to $V_0$. This is explained by the phenomenon fact that the response evoked by a pulsatile stimulus represents a non-steady state

response. The relationship between various values of $i(t)$ at a steady $I_0$ and $V(t)$ defines the contrast sensitivity.

In the experiment for which results are shown in Fig. 1 *A1*, the mean illuminance was modulated with a 3-Hz sinusoidal input at modulation depths that ranged from 4 to 88% in five steps. The resulting modulation response from the horizontal cell was a 3-Hz sinusoid and the amplitude of the modulation response appeared to be proportional to the depth of the input modulation; such that $V(t)$ was approximately proportional to $I(t)$ . The maximal amplitude of the modulation response was 25 mV, a value similar to that found in turtle horizontal cells. Fig. 1 *A* shows quantitatively that the depth of the modulation of the response increased linearly with the increase in the modulation of the input.

Fig. 2 shows two sets of first-order kernels from a horizontal cell of a kissing gourami upon a simultaneous stimulation by a red (*A*) and a green (*B*) light that were

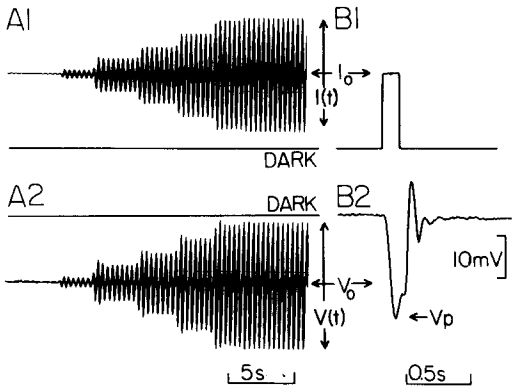


FIGURE 1. Recordings from a luminosity horizontal cell of the kissing gourami. The response was evoked by a red field of light. (*A1*) Input modulated by a 3-Hz sinusoid with the depth of modulation ranging from 4 to 87%. (*A2*) Resulting modulation response from the horizontal cell. (*A1* and *A2*) an input $I_0$ produced a steady hyperpolarization, $V_0$, and modulation of the mean, $i(t)$, produced a modulation response, $V(t)$. (*B1* and *B2*) Pulsatile input with an amplitude of $I_0$, the mean of the modulation input in *A1* and the resulting response, which is characterized by transient phases at the on and off set of the pulsatile input. The responses from the horizontal cell of the kissing gourami are characterized by overshoots at the on and off sets of pulsatile stimulus. The horizontal cells of the gourami are similar to the horizontal cells in the turtle retina (Chappell et al., 1985).

modulated by two independent white-noise signals. Modulation depths were set to 25, 35, and 70%. In spite of the differences in the depth of modulation, the kernels evoked by red and by green lights were similar in terms of amplitude as well as waveform. The kernels evoked by the green input (Fig. 2 *B*) were more oscillatory than those evoked by the red input (Fig. 2 *A*) at all depths of modulation. This observation shows that the response dynamics were also invariant of the depth of modulation. The mean square error (MSE) of the predictions, linear models, by the red and green (first-order) kernels was between 4 and 9%. For a physiological system, this degree of linearity of a response whose amplitude is $>20$ mV (Fig. 2 *D*) is quite extraordinary (Winslow and Ma, 1990).

In a linear system, the PDF of the output, the response, is Gaussian. In the case of horizontal cells, a white-noise modulation produced a response whose PDF is closely fitted by a Gaussian function. One example is shown in Fig. 2 *C* (*input*) and D

(*output*). PDFs (*noisy traces*) for the inputs and outputs are fitted with Gaussian functions (*smooth traces*). Indeed, the two sets of PDFs could be superimposed on one another. These two pieces of evidence, one from the waveform of the kernels as well as the small MSE of the predicted response and the other from the Gaussian distribution of PDFs, show that the modulation response from a horizontal cell is linearly related to the depth of modulation. Therefore, the contrast sensitivity, as defined by the first-order kernels, is independent of the depth of input modulation. The horizontal cell shows a piece-wise linearization in that, at a steady state, the cell's response is linear over a range of modulation depths. Similar observations were made

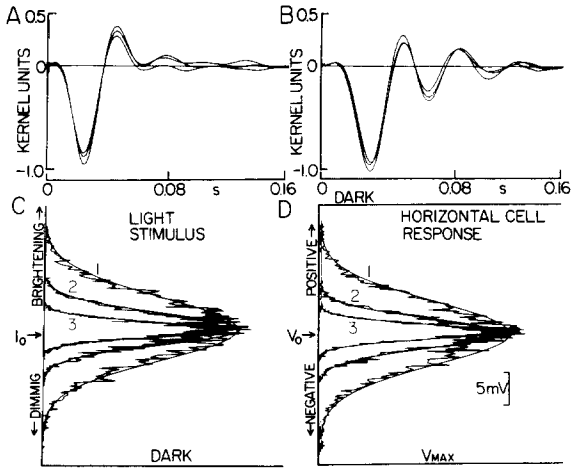


FIGURE 2. Modulation responses from a horizontal cell in a kissing gourami. Responses were evoked by two superimposed inputs, red and green, and the resulting response was decomposed into red and green components through a process of cross-correlation, two-input and one-output experiment, (Marmarelis and Naka, 1974). The mean luminance, $I_0$ for the red input, was modulated by white-noise signals whose PDFs are shown in C in which curves marked 1, 2, and 3 correspond to a depth of modulation of 25, 35, and 70%, respectively. (*D*) PDFs of the resulting responses evoked by the red inputs are shown. (*C* and *D*) All experimental curves are fitted with the best-fitting Gaussian function. For both input and output PDFs, the fit is good. (*A*) The response was evoked by a red input; and (*B*) the response was evoked by a green input, the first order kernels are shown. Two sets of kernels, generated by red and green inputs of different depths of modulation have identical waveforms and amplitude. The modulation response was linear and, as a logical consequence, there was no contrast gain control. Kernel units, 1.0, are $1.3 \times 10^{-7}$ mV photons$^{-1}$ mm$^2$ s$^{-1}$ for the red kernels, Fig. 2 *A*, and $0.8 \times 10^{-7}$ mV photons $^{-1}$ mm$^2$ s$^{-1}$ for the green kernels, Fig. 2 *B*. Note that when light is made brighter the potential becomes more hyperpolarized (negative) because the polarity of the kernel is negative, i.e. sign reversing.

in the cones and horizontal cells of the turtle (Chappell et al., 1985; Naka et al., 1987), in the ocellar neurons of the cockroach (Mizunami et al., 1986), in the horizontal cells of the skate (Naka et al., 1988), and in the horizontal and bipolar cells of the catfish (Sakai and Naka, 1987*b*).

### *N Amacrine Cells*

Control of contrast sensitivity in the N (sustained) amacrine cells is very different from that in the horizontal cells. In the N amacrine cells, contrast sensitivity is greater for an input of smaller depth of modulation. Fig. 3 shows two sets of responses from

an NB amacrine cell of the catfish, which correspond to the sustained hyperpolarizing amacrine cells in other retinas (cf. Kaneko, 1970). Responses were evoked by a large field of red light that was modulated by two white-noise signals, one with a modulation depth of 6% (Fig. 3 *A1*) and the other with a modulation depth of 80% (Fig. 3 *B1*), while $I_0$ was kept constant. PDFs of the inputs and outputs are also shown in Fig. 3 *A1* and *B1*. The response evoked by the input of smaller modulation was 10 mV, peak-to-peak, whereas the response evoked by the input of larger modulation was 15 mV, as shown by the time records as well as by the response PDFs. The amplitude of the PDFs of the inputs differed by a factor of 10, whereas the difference was less than a factor of 2 for the response. We note that the response PDF produced by a smaller input is more like a Gaussian curve while that produced by a larger input is strongly skewed (distorted as compared to a Gaussian curve), revealing the

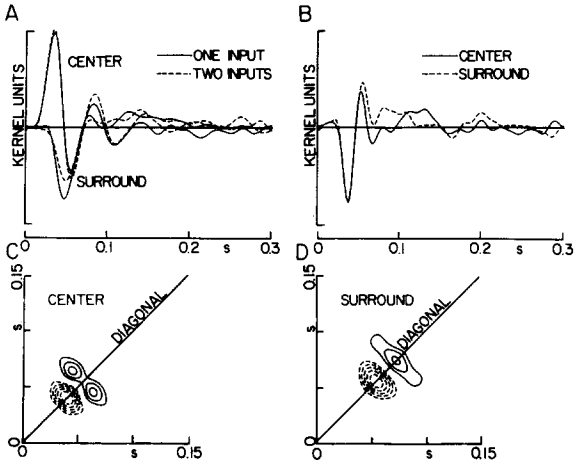


FIGURE 3. Responses from an NB (sustained hyperpolarizing) amacrine cell of a catfish evoked by modulations of a mean luminance. (*A1*) The depth of modulation of the input was 6%, whereas in *B1* it was 80%. The resulting responses are shown in *A2* and *B2*. The PDF of the response (*A2*) evoked by the small modulation was close to a Gaussian distribution whereas the response PDF (*B2*) evoked by the large modulation was highly skewed (distorted from the input Gaussian distribution). This distribution reveals the presence of a large nonlinear component, a transient depolarization, evoked by the modulation input, as seen in the time record. N amacrine cells of both the catfish and the kissing gourami produce a marked transient response to modulation of an input (Sakai and Naka, 1987*a*,*b*). $I_0$ shows the mean luminance.

presence of a strong nonlinear component (McKean, 1973; Bendat, 1990). In the time record, the nonlinearity is shown by many transient depolarizing peaks that are characteristic of the N cells of the catfish (Sakai and Naka, 1988). The cell shown here was one of the minority of cells whose response evoked by a stimulus of small depth of modulation was nearly linear. The results in Fig. 3 show quantitatively that the cell's contrast (incremental) sensitivity, unlike that of the horizontal cells, depends upon the depth of modulation. This NB cell's modulation response is apparently different from the cell shown in Fig. 5.

Fig. 4 shows a series of responses recorded from an NA (sustained depolarizing) amacrine cell of the catfish. In the experiments from which results are shown in Fig. 4*A*, the stimuli were (*a*) a flashing spot of light in the presence of steady annular illumination; (*b*) a flashing annulus in the presence of steady spot illumination; or (*c*)

the spot and annulus flashing together in dark. The steady spot illumination depolarized the cell with an accompanying 35-Hz oscillation whereas steady annular illumination hyperpolarized the cell. In the dark, the resting potential settled somewhere between the levels evoked by steady center and steady surround illumination, respectively. The NA amacrine cell shows a concentric receptive field, as

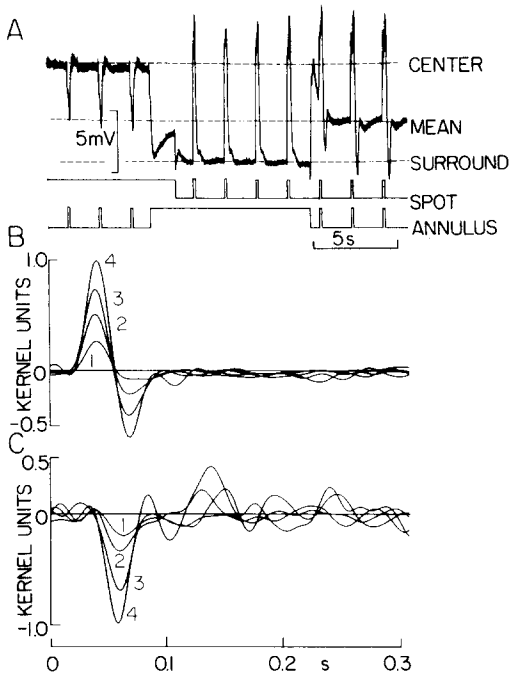


FIGURE 4. Recordings from an NA amacrine cell of a catfish. A shows pulsatile responses evoked by a combination of a steady spot or steady annular illumination and a pulsatile spot or annular stimulation, as shown by the two lowest traces. Steady spot illumination depolarized the cell to the level marked *center* and an annulus of light produced a hyperpolarizing response marked *surround.* The thick baseline, seen during steady spot illumination, shows the characteristic 35-Hz oscillation. As seen in the middle part of the record, a steady annular illumination produced a steady hyperpolarization and a pulsatile spot produced large depolarizing responses. Simultaneous stimulation by the spot and annular inputs produced a large depolarization followed by an after-hyperpolarization, characteristic of the response from the catfish NA cells to a pulsatile input given in the dark. Note that, in the dark, the membrane potential settled down, as indicated by *mean,* somewhere between two levels, namely, *center,* produced by steady spot illumination, and *surround.* In the presence of steady spot and annular inputs, as in the case of two-input white-noise stimulation, the membrane potentials also settled down at close to the level shown by *mean.* (*B* and *C*) The results of a two-input white-noise experiment in which the spot and annulus were modulated by two independent white-noise inputs and the spot kernels (*B*) and annular kernels (*C*) were computed by cross-correlating two inputs against one output. Modulation depths were 80% for the kernels marked 1, 35% for the kernels marked, 2, 15% for the kernels marked, 3, and 7% for the kernels marked, 4. All kernels evoked by the spot inputs (*B*) had same peak-response times as did the annulus-evoked kernels (*C*). The peak-response times of spot and annular kernels differed by 20 ms, as noted previously by Sakai and Naka (1992). $I_0$ for the spot and annular inputs were $1.6 \times 10^9$ and $7 \times 10^8$ photons $mm^{-2}$ $s^{-1}$. Kernel units, 1.0, are $6 \times 10^{-6}$ mV photons$^{-1}$ $mm^2$ $s^{-1}$ for the spot kernel and $1.2 \times 10^{-6}$ mV photons$^{-1}$ $mm^2$ $s^{-1}$ for the annular kernels.

revealed by steady illumination of the receptive-field center or surround and as demonstrated previously by Sakai and Naka (1992). Next, we used a spot and an annulus of light that were modulated by two independent white-noise signals, in other words, the receptive-field center and surround were simultaneously stimulated. The resulting response was decomposed into the spot and annular components by

cross-correlation between two inputs and one output. The kernels generated by the spot inputs were an initial depolarization followed by a hyperpolarization phase (Fig. 4 *B*) and the kernels generated by the annular inputs were hyperpolarizing (Fig. 4 *C*), i.e., the receptive-field organization was encoded by the DC (0th-order) component, (Fig. 4 *A*), as well as by the first-order components (Sakai and Naka, 1992). There was a 20-ms transport delay between the center and surround kernels. The depth of modulation of the two stimuli was changed over four intervals from 80% (kernels marked 1), to 7%, (kernels marked 4). The first-order kernels evoked by the spot and annular stimuli were both larger for the smaller modulation and smaller for the

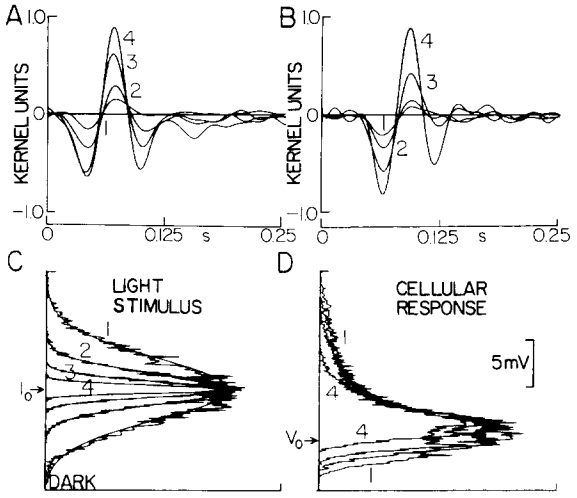


FIGURE 5. Recordings from an NB amacrine cell of a catfish. (*A*) Kernels generated by the spot input and (*B*) kernels generated by the annular input. Responses were evoked by a spot and annular inputs modulated by two independent white-noise signals. The resulting response was decomposed into the spot and annular components by cross-correlating the two inputs against one output. The first-order kernels generated by the spot input were mostly triphasic and those evoked by the annular input were also triphasic. Kernels marked by 1, 2, 3, and 4, were generated by modulation depths of 82, 43, 20, and 9%, respectively (*C* and *D*) The PDFs of the inputs and outputs. Input PDFs marked 1 through 4 generated output PDFs marked 1 through 4 (two output PDFs' 2 and 3 are unmarked). The input PDFs are Gaussian but the output PDFs are highly skewed, showing the presence of transient depolarizing peaks characteristic of the catfish N amacrine cells, one example of which is shown in Fig. 3 *B2*. $I_0$ and $V_0$ show the approximate levels of mean illuminance and the membrane potential in the presence of spot and annular inputs. The membrane potential, $V_0$, was similar to that seen in the dark and was −15 mV. Kernel units, 1.0, are $1.3 \times 10^{-7}$ mV photons$^{-1}$ mm$^2$ s$^{-1}$ for the spot kernel and $1.1 \times 10^{-7}$ mV photons$^{-1}$ mm$^2$ s$^{-1}$ for the annular kernels.

larger modulation. The linear part of the NA cell's response, for both the receptive-field center and surround, shows contrast gain control that is roughly similar for the center and surround of the field. The kernels in each set had similar waveforms and they could be superposed, when they are normalized in respect to their amplitude, on top of one another as shown in Fig. 8 *B2*. There was no change in the dynamics of the linear component derived from a center or a surround of a receptive field.

The results shown in Fig. 5 were obtained from a catfish NB amacrine cell with the same stimulus configuration as that were used to generate the results in Fig. 4, namely, the receptive-field center and surround were stimulated simultaneously by a

spot and an annulus of light, which were modulated by two independent white-noise signals. The spot and annular inputs produced first-order kernels with complex waveforms. The kernels are predominately triphasic and the spot and annular kernels differ in their latency; there is a transport delay of ~20 ms between the two sets of kernels. The kernel marked 1 was evoked by stimulation with a depth of modulation of 82% whereas the kernel marked 4 was evoked by a stimulus with a 9% modulation. As in the NA amacrine cell for which results are shown in Fig. 4, the contrast gain was dependent upon the depth of modulation. Fig. 5, *C* and *D*, shows the PDFs of the spot inputs and outputs. The input and response PDFs marked 1 correspond to the largest modulation, 82%, of the signal and those marked 4 to the smallest modulation, 9%, of the signal. Obviously the PDFs of the input were Gaussian whereas those of the response were highly skewed, indicating that the response had nonlinear components. The comparison of the PDFs for the horizontal cells shown in Fig. 2 and those shown here is striking. In the NB cells for which

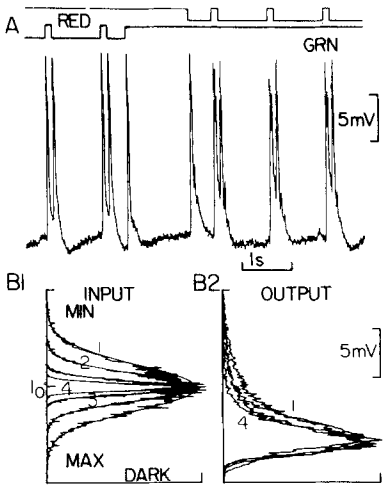


FIGURE 6. Responses from a C amacrine cell of a kissing gourami. (*A*) The cell's response to a field of either red or green light modulated by pulsatile inputs. The cell produced a transient depolarization when there was a change in the input, namely, brightening, dimming, or pulsatile red or green inputs. (*B1* and *B2*) The PDFs of inputs and outputs. The modulation depth of inputs ranged from 10 to 90% and input PDFs were fitted to Gaussian functions shown by smooth solid lines. The output PDFs all exhibited a similar and skewed distribution irrespective of the depth of modulation of the input.

results are shown in Fig. 5, the amplitude of the modulation response, as shown by the PDF, decreased from 17 mV (trace *1* in Fig. 5 *D*) to 9 mV (trace *4*) when the depth of modulation of the stimulus was decreased from 82 to 9%: an almost 10-fold change in the depth of modulation only halved the response amplitude. This difference corresponds to a fivefold increase in the contrast sensitivity. All response PDFs had a similar skewed distribution, showing: (*a*) the response contained a strong nonlinear component which produced sharp depolarizing transients (Fig. 3 *B2* in this paper and Fig. 3 in an earlier paper by Sakuranaga and Naka, 1985); and (*b*) the nonlinearity was produced even by an input with a small depth of modulation.

### *C Amacrine Cells*

One class of amacrine cells consists of transient amacrine cells. Fig. 6 *A* shows the time record for a series of responses from a transient amacrine cell in the retina of a kissing gourami. The cell's morphology was characterized by its two-layered dendritic

fields, one in the distal layer of the inner plexiform layer (IPL) and the other in the proximal layer of the IPL (Naka and Ohtsuka, 1975; Sakai and Naka, 1988). The C amacrine cells of the gourami fish produce transient depolarization when there is a change in luminance, whether dimming or brightening, or when there is a red or a green input. As in the C amacrine cells of the catfish, steady illumination did not generate any change in the membrane potential (Fig. 6 *A*). Results of white-noise stimulation are shown in Fig. 6 *B1*, for the inputs, and Fig. 6 *B2*, for the outputs, as PDFs. The depth of modulation was 80% for the PFD marked 1 and 10% for the PDF marked 4. The input PDFs are Gaussian, as we would expect, but the PDFs of the output response all show a skewed distribution and the four PDFs produced by inputs of various depths of modulation are almost identical in their distribution characteristics. Two conclusions can be drawn, as follows: (*a*) the contrast sensitivity increased as

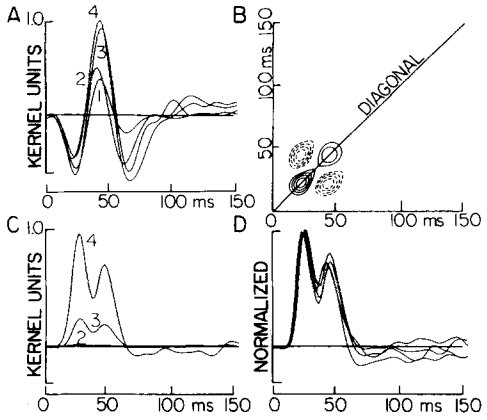


FIGURE 7. The first- and second-order kernels from the C amacrine cell for which data are shown in Fig. 6. (*A*) The first-order kernels for the inputs whose PDFs are shown in Fig. 6 *B1*. The amplitude of kernels, the contrast sensitivity, differed only by 30% while the range of input modulations varied from 80 to 10%. (*B*) A topographic representation of the second-order kernel obtained for an input with a depth of modulation of 80%. The kernel has a characteristic four eye structure but is slightly filtered, as seen from the elliptic shape of each of the four eyes. (*C*) Four second-order kernels as their diagonal cuts. The largest kernel was associated with a stimulus with 10% modulation and the smallest with 80% modulation. In *D*, all diagonal cuts in *C* have been normalized in terms of amplitude. Kernel units, 1.0, are $1.6 \times 10^{-7}$ mV photons$^{-1}$ mm$^2$ s$^{-1}$ for the first-order kernel and $2.4 \times 10^{-17}$ mV photons$^{-2}$ mm$^4$ s$^{-2}$ for the second-order kernel.

the depth of modulation becomes smaller, and (*b*) smaller signals did not change the nonlinear characteristics or linearize the response, as is also the case in N amacrine cells (Fig. 5).

Fig. 7 shows the first- and second-order kernels from the input and output shown in Fig. 6. In both the catfish and the kissing gourami the linear component of the modulation response from a C amacrine cell is small. The linear component accounts for $< 10\%$ of the total response in terms of MSE whereas the second-order component accounts for $> 50\%$ of a cell's response in terms of MSE. The four first-order kernels shown in Fig. 7 *A* do not differ much in their amplitude, by contrast to the similar kernels from N amacrine cells shown in Figs. 4 and 5. We do not know how general these results might be because the first-order kernels from C amacrine cells are often noisy as one would expect from the component's small

contribution to the total response. Fig. 7 *B* shows a topographic view of the second-order kernel obtained from an input with a depth of modulation of 80%. The kernel has a characteristic signature, namely, a four-eye signature, showing that the nonlinearity was probably generated by a cascade of the Wiener type, in which a dynamic linear filter is followed by a static nonlinearity equivalent to squaring (cf. Figs. 16 and 17 in Sakai and Naka, 1987*b*). Fig. 7 *C* shows the diagonal cuts of the second-order kernels generated by inputs with different depths of modulation (Fig. 6 *B1*). With a decrease in the depth of modulation from 80 to 10%, the amplitude of the second-order kernel increased by a factor of 50. In Fig. 7 *D*, the diagonal cuts are normalized in terms of amplitude and all cuts were superposed on top of one another. It appears, therefore, that; (*a*) there is control of contrast involving the second-order components, with the change in the contrast gain being much greater

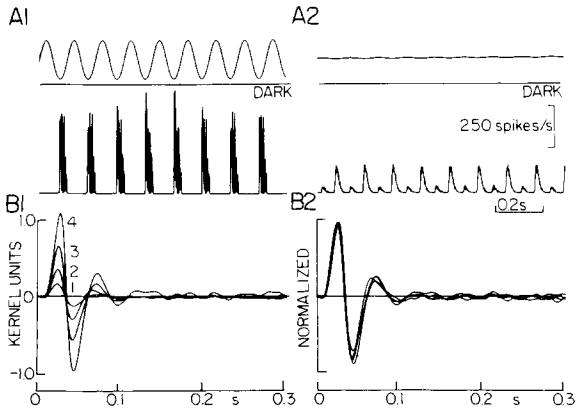


FIGURE 8. A spike train from a ganglion cell of a catfish. (*A1* and *B1*) PST histograms of discharges evoked by a 5-Hz sinusoidal input. (*A1*) The depth of modulation was 80% and in *A2* it was 6%. (*A1*) the large modulation produced a PST histogram that resembled the sum of individual discharges, each discharge being time locked to the stimulus. The generation of the histogram failed to reveal a smooth response, as seen in the study by Korenberg et al. (1990). (*A2*) The histogram is smooth and doubling of the frequency is seen visible. (*B1* and *B2*) The first-order kernels generated by stimuli with different depths of modulation. Kernels marked 1, 2, 3, and 4 were generated by stimuli with the depths of modulation of 80, 45, 15, and 8%, respectively. (*B2*) Kernels were normalized to show that, in spite of the large difference in their amplitudes, the wave-forms of the kernels were invariant. Kernel units, 1.0, are $3.9 \times 10^{-7}$ spikes photons$^{-1}$ mm$^2$ s$^{-1}$.

than in the case of the linear component; and (*b*) in spite of the large difference in the contrast sensitivity, the response dynamics of the second-order components do not change much. The contrast gain for the second-order component is roughly a quadratic function of that for the first-order component as shown in Fig. 10.

*Spike Discharges*

Fig. 8 shows the results of modulation experiments performed on spike discharges from on-center ganglion cells. Fig. 8 *A1* and *A2*, shows the PST histograms of discharges evoked by a 5-Hz sinusoidal input. The depths of modulation for Fig. 8, *A1* and *A2* were 80 and 6%, respectively. When the depth of modulation was large, generation of spike discharges was synchronized or phase-locked to the stimulus and the histogram had a rugged contour (Korenberg et al., 1990). Smaller modulations

produced a smooth and frequency-doubling PST histogram (Fig. 8 *A2*). These two histograms demonstrate, as already shown in an NB amacrine cell, Figs. 3 and 5, that: (*a*) the neurons in the retina produce a well-defined response to a modulation of ~6%; and (*b*) the frequency-doubling (static) nonlinearity is evident even in the response evoked by a stimulus of very small depth of modulation. Fig. 8, *B1* and *B2*, show the first-order kernels obtained at four levels of modulation, ranging from 80%, trace marked *1*, to 10%, trace marked *4*. The amplitude of the kernels, and hence, the contrast sensitivity, is larger for the smaller modulation stimulus than for the larger modulation stimulus. In Fig. 8 *B2*, kernels are normalized with respect to amplitude; in spite of a fivefold increase in contrast sensitivity, the waveform of the kernels remains unchanged since they match with one another almost perfectly, in other words, there was no change in the response dynamics of the linear component.

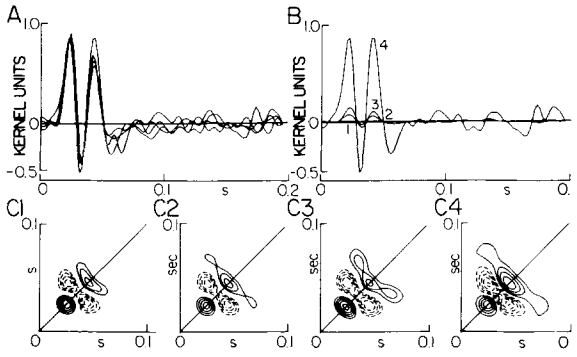


FIGURE 9. Second-order kernel from the spike train whose first-order kernels were shown in Fig. 8. A shows the normalized diagonal cuts of the second-order kernels generated at four different depths of modulation. The waveforms are almost identical. (*B*) The diagonal cuts plotted on an incremental- or contrast-sensitivity scale. The cut marked 4 was derived from stimulation with a depth of modulation of 8%. Note that the increase in the amplitude of the kernels is much more dramatic than in the case of the first-order kernels. (*C1–C4*) The second-order kernels generated by stimuli with four depths of modulation, as in Fig. 6. (*C1–C4*) correspond to depths of modulation of 80, 45, 15, and 8%, respectively. Diagonal cuts of these kernels are shown in *A* and *B*. Kernel units, 1.0, are $1.5 \times 10^{-12}$ spikes photons$^{-2}$ mm$^4$ s$^{-2}$.

Fig. 9 shows the second-order kernels obtained from the data shown in Fig. 8. Fig. 9 *C1–C4* show four second-order kernels generated by four inputs with modulation depths of 80% (*C1*), 45% (*C2*), 15% (*C3*), and 8% (*C4*). The kernels all show the distinct signature of a nonlinearity generated by an NB amacrine cell (cf. Fig. 9 in Sakai and Naka, 1987*a*). The kernels' characteristics are (*a*) a valley, a decrease in spike frequency, sandwiched between two peaks, an increase in the spike frequency; and (*b*) elongation of the peak and valley orthogonal to the diagonal. Four second-order kernels obtained at four levels of modulation have a similar signature but those obtained at smaller depths of modulation seem less tightly structured. We made diagonal cuts of three-dimensional kernels shown in Fig. 9, *C1–C4*. When normalized with respect to their amplitude, the cuts are all similar in their waveform, showing that the dynamics of second-order components, at least as indicated by the diagonals, were similar regardless of the depths of modulation (Fig. 9 *A*). In Fig. 9 *B*, the diagonal cuts are shown with a contrast sensitivity scale. It can easily be seen that the amplitude of the kernel, marked 4, evoked by a smaller modulation input was

much larger than that of the kernel, marked 1, evoked by a larger modulation (cf. Fig. 10 *B*). The difference in the amplitude of the kernel is much larger than was observed in the case of the first-order kernels (Fig. 8 *B1*). When the depth of modulation was decreased from 80 to 10%, the amplitude of the first-order kernel increased sixfold whereas the increase for the second-order kernel was 58-fold. Several conclusions can be drawn from the observations in Figs. 8 and 9, as follows: (*a*) the linear part of the response of a ganglion cell shows contrast gain control similar to that seen in the amacrine cells; (*b*) a small input does not linearize a response nor markedly change the second-order dynamics; and (*c*) the increase in the contrast sensitivity is much greater for the second-order component than for the first-order kernel.

*Summary of Results*

In Fig. 10 *A* the amplitude of the first-order kernel is plotted against the depth of modulation. In the plot, the amplitude of the kernel at a modulation depth of 80 to

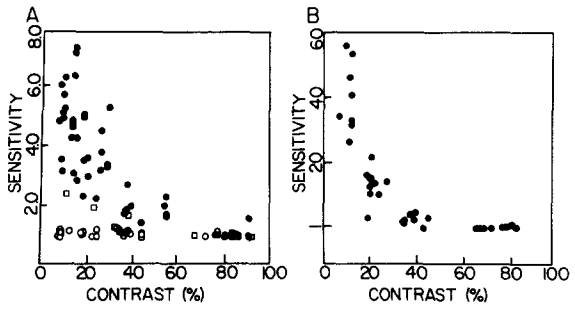


FIGURE 10. The relationship between the depth of modulation and normalized contrast gain, as indicated by the amplitude of the first-order kernels (*A*) and that of the second-order kernels (*B*). The amplitude of the kernels generated by the largest contrast, namely, at modulation depths of 80–90%, is taken as unity. (*A, open circles*) Correspond to the horizontal C amacrine cells.

90% is taken as unity. Data are from horizontal cells ($n$ = 8), N amacrine cells ($n$ = 12), C amacrine cells ($n$ = 4), and spike discharges ($n$ = 7). The horizontal cells' contrast sensitivity, shown by open circles in Fig. 10 *A*, remained unchanged when the depth of modulation was changed from 90 to >10%. However, the contrast sensitivity of N amacrine cells and ganglion cells (spike discharges), both shown by filled circles, increased as the depth of modulation decreased. Such increases in sensitivity ranged from threefold to nearly eightfold at a depth of modulation of ~10%. The considerable scattering of the filled circles shows that there were differences in the increase in sensitivity from cell to cell. No difference was apparent between the amacrine and ganglion cells. The contrast gain of the C amacrine cells, shown by open squares in Fig. 10 *A*, remained fairly constant and the increase varied between one- and twofold.

A similar plot for the second-order kernel from amacrine (intracellular response) and ganglion (extracellularly-recorded spike discharges) cells is shown in Fig. 10 *B*. The increase in contrast sensitivity of the second-order component, as indicated by the amplitude of the second-order kernels from N amacrine and ganglion cells was 30- to nearly 60-fold at a depth of modulation of ~10% (Fig. 10 *B*). The greater

increase in the contrast sensitivity for the second-order component than for the first-order component indicates that the control of contrast sensitivity occurred before the generation of the nonlinearity (see Appendix; Wang and Naka, manuscript in preparation).

## DISCUSSION

In this study we examined the retinas of the channel catfish and of the kissing gourami. Under our experimental conditions, only one class of cones appears to be active in the catfish, while two classes of cones are active in the gourami retina. The two preparations are, therefore, complementary. The interpretation of our data from the gourami retina is based on an extensive functional and morphological study (Sakai, Machuca, and Naka, manuscript in preparation). The catfish retina is one of the few retinas in which network functions including dynamics of light-evoked response as well as of signal transmission between neurons have been extensively studied and analyzed (Naka and Sakai, 1991). For example, in the catfish retina, the nonlinearity carried by a spike train has been traced back to a particular class of amacrine cells (Fig. 9 in Sakai and Naka, 1987*a*).

Classically, two kinds of adaptation have been defined: bleaching adaptation and field adaptation, the former being a dimming of dark light and the latter being related to a steady background light (Rushton, 1965). In addition to these two classical types of adaptation, Shapley and Victor (1979, 1980, 1981) discovered a third type of adaptation, which they called contrast gain control. Shapley and Victor (1979, 1980, 1981) found that ganglion cells were more sensitive to modulations of smaller amplitude than to those of larger amplitude. In both the cat and monkey, the contrast gain control is activated primarily by stimuli of high temporal frequency, but shows a suppressed response to low temporal frequency thus demonstrating that the control is frequency dependent. This dependence of response dynamics on the depth of modulation is less evident in the P cells than in the M cells of the monkey (Benardete et al., 1992).

Shapley and Victor (1981) and Victor (1987) proposed a model to account for the changes in the gain as well as in the dynamics of cat X and Y cells with changes in the depth of modulation: they proposed that the response was more transient and less sensitive for an input with a larger depth of modulation. In their model, several stages of low-pass filters are followed by a single stage of negative feedback. Contrast and peripheral stimulation change the parameters of the model in a similar fashion. Another view is that the automatic gain control that regulates the contrast sensitivity of a receptive field center is localized at the center and, thus contrast is computed only locally (Shapley and Enroth-Cugell, 1984). In this study, we took advantage of the fact that a Wiener kernel is a measure of incremental sensitivity that includes response dynamics (Naka et al., 1979; Sakuranaga and Ando, 1985). Contrast sensitivity is defined as the incremental sensitivity around a given mean luminance; the parameter that changes is the depth of modulation.

Our results from horizontal cells were what we might have expected from previous studies of similar cells in retinas of the turtle (Chappell et al., 1985; Naka et al., 1987), catfish (Naka and Sakai, 1988), and skate (Naka et al., 1988). These results and the present results show that the modulation responses from a horizontal cell at

a given mean luminance, i.e., at a steady state, are linear. Moreover, the fact that the first-order kernels obtained by stimuli with various depths of modulation were identical in their amplitude as well as waveform provides further evidence to show the linearity of the cell's modulation response. The linearity was maintained even when the retina was stimulated simultaneously with two inputs of different color. What we have seen in the horizontal cell is a piecewise linearization; when mean changes sensitivity as well as dynamics changes.

The contrast gain control we have observed found in both catfish and gourami fish can be modeled by a simple cascade of Wiener type (Korenberg, 1973) in which the static nonlinearity is an amplitude saturation. This is shown in Fig. 11 in which the first-order kernels from the horizontal cell of a kissing gourami were obtained at five modulation depths, 80, 60, 40, 20, and 10%. As already shown in Fig. 2, the kernels are all similar in terms of amplitude as well as waveform. The original responses

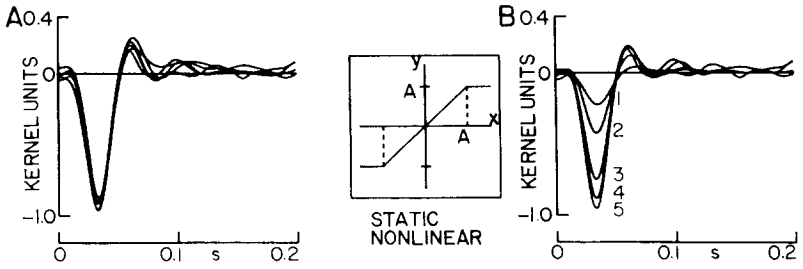


FIGURE 11. *A* shows five kernels from a horizontal cell in kissing gourami generated by white-noise inputs with modulation depths of 80, 60, 40, 20, and 10%, respectively. As shown in Fig. 2, the kernels evoked by inputs of different depths of modulation are almost identical in their waveforms as well as amplitudes. (*B*) The kernels from the same set of response shown in A but computed after the responses had been convolved with a saturation-type static nonlinearity. Kernels marked 1 through 5 were generated by white-noise inputs with modulation depths of 80–10%. The box between the two sets of kernels provides a schematic representation of the saturation-type nonlinearity. *A* in the box denotes the levels of saturation, which corresponds to the two saturation levels ($-A$ and $A$) in Fig. 14.

obtained with modulated stimuli were convolved through a saturating nonlinearity and a new set of kernels was computed by cross-correlating the original inputs against the output of the saturating device. The resultant kernels, shown in Fig. 11 *B*, are different in their amplitude, i.e., the kernels generated by smaller modulations are larger and those generated by larger modulations are smaller as we have observed in the amacrine cells and ganglion cells (Figs. 4, 5, and 8). As would be expected from the static nature of the nonlinearity, the original (from catfish horizontal cell) and transformed kernels are identical in their waveforms. The PDF of the model responses predicated by the transformed kernels is Gaussian. The static nonlinearity changes only the amplitude of the kernels. The Appendix provides a short mathematical proof of the model.

The naming of this mechanism in the lower vertebrate retinas as automatic gain control is an objective choice. The saturating nonlinearity must be located between

the outer and inner retinas and we speculate that it might exist between the bipolar and amacrine cells since we found no marked contrast gain control in the bipolar cells (Sakai and Naka, 1988). This mechanism operated on both the receptive-field center and the surround (Figs. 4 and 5). The saturating nonlinearity did not affect the nature of the second-order nonlinearity but operated on the amplitude of the second-order kernel, which increased more steeply than the linear component, in an approximately quadratic fashion. An exception exists, that is, the linear component from the C amacrine cell. The component did not change its amplitude, as the N amacrine cell did, when the depth of modulation was changed, whereas the second-order component did. We do not know why this is so. The linear component in the C cell's response is similar to the linear component of the bipolar cell, and is less complex than the linear component of the N amacrine cell.

What are the implications of contrast gain control? First, it allows the network better detection of smaller modulations. In our experiments, the smallest modulation that gave a well defined kernel was 4–6% but this value can probably be reduced with more sensitive detection of input signals. We estimate that the smallest modulation that fish can detect is $\sim 1\%$. This value is about five times larger than that reported as the minimal detectable contrast in human psychophysics studies (Lawton and Tyler, 1993). Second, the inverse relationship between the depth of modulation and the contrast gain renders the amplitude of the response less dependent upon the amplitude of the modulation, as can easily be seen by comparing PDFs for horizontal cells in Fig. 2 with the PDFs for an amacrine cell in Fig. 5. In the horizontal cells, large modulations evoked large modulation responses that could be more than 20 mV peak-to-peak in some cells. In the amacrine cell, the amplitude of the PDF differed by a factor of 2, while the depth of modulation was varied from 80% to $< 10\%$. Neurons in the inner retina do not generate a large analogue response as horizontal cells do. There has to be a mechanism to equalize or compress the large modulation response generated in the outer retina, in particular in the horizontal cells. This mechanism is equivalent to automatic contrast gain control.

A simple saturating nonlinearity produces complex phenomena, one example of which is shown in Fig. 12. Recordings were made from an N amacrine cell of a kissing gourami, whose response to a pulsatile input is shown in Fig. 11 *A*. The cell produced a biphasic linear kernel and an NB-type second-order kernel (Sakai and Naka, 1987*a*). In the experiment for which results are shown in Fig. 12 *B*, the input was a 10-Hz sinusoid, the amplitude of which was suddenly reduced. For $\sim 0.5$ s, the sudden decrease in the modulation depth failed to produce any response from the cell. Apparently, generation of a modulation response is a complex process. Neurons in the inner retina produce responses with different proportions of linear and nonlinear components (cf. Fig. 10 in Sakai and Naka, 1987*a*). Here we have shown that control of contrast sensitivity for the second-order components is approximately a quadratic function of similar control for the first-order component. Thus control of contrast gain involving a different ratio of linear and nonlinear components can produce a very complex response from the neurons in the inner retina. It may be that a combination of many simple static nonlinearities contribute to the generation of complex modulation responses. In the past we have suggested that the generation of the transient response from the C amacrine cell could be modeled by a simple Wiener

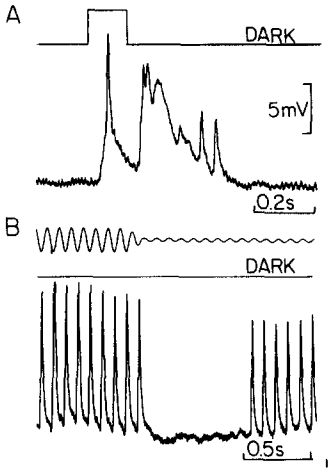


FIGURE 12. Recordings from an NB amacrine cell of a gourami. This cell was identified as an NB amacrine cell based on the basis of its morphology, as well as the polarity of the first-order kernel and the signature of the second-order kernel. (*A*) Response evoked by a pulsatile input. (*B*) Cell's response to a sinusoidal modulation of 10 Hz and a depth of 30% which was suddenly decreased to 8%.

cascade in which a dynamic linear filter was followed by a static nonlinearity that was approximated by a simple squaring device (Sakai and Naka, 1987*b*). Generation of spike discharges in the ganglion cell is highly nonlinear but approximately static (Korenberg et al., 1989). Our white-noise analyses of retinal neuron network have shown that many types of static nonlinearity play important roles in network function.

## APPENDIX

### *Wiener Kernels of a Saturated Linear System*

A saturated linear system is equivalent to a dynamic linear system, $h(t)$, followed by a static nonlinearity, $g(.)$, which is a clipping or saturating nonlinearity (Fig. 13). This system is a cascade structure of the Wiener type (Korenberg, 1973): where

$$x(t) = \int_0^\infty h(\tau)u(t-\tau)\,d\tau, \tag{A1}$$

$$g(x) = \begin{cases} -A & x < -A \\ x & |x| \le A \\ A & x > A \end{cases}. \tag{A2}$$

For a Gaussian white noise, GWN, input $u(t)$ with variance $\sigma_u$, the linear response $x(t)$ also has a Gaussian distribution whose PDF, $p(x)$, is:

$$p(x) = \frac{1}{\sigma_x\sqrt{2\pi}} e^{-(x^2/2\sigma_x^2)} \tag{A3}$$

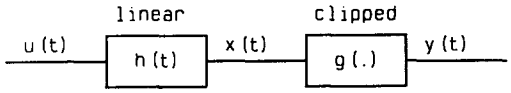


FIGURE 13. A cascade structure of the Wiener type in which a linear dynamic filter, $h(t)$, is followed by a static nonlinearity, $g(\cdot)$, that is equivalent to clipping or saturation. Kernels shown in Fig. 11 *A* were obtained by cross-correlating the input white noise, $u(t)$, against the output of the linear filter, $x(t)$. Kernels in Fig. 11 *B* were obtained by cross-correlating the white-noise input, $u(t)$, against the output of the cascade, $y(t)$.

and its variance $\sigma_x$ is given by the equations:

$$\sigma_x^2 = \langle x^2(t) \rangle = \sigma_u^2 \int_0^\infty h^2(\tau)\, d\tau, \tag{A4}$$

where $<\cdot>$ denotes the time average.

The clipping or saturation, $g(.)$, is a zero-memory nonlinearity. For a Gaussian input, $x(t)$, according to Bussgang's theorem (Bendat, 1990), the optimum linear system $K_1(f)$ for this nonlinear $g(.)$ is given by:

$$K_1(f) = \frac{\langle xg(x) \rangle}{\sigma_x^2}. \tag{A5}$$

The transfer function, $K_1(f)$, is frequency-independent because the $g(x)$ transformation has no memory. The Gaussian distribution of variable $x(t)$ yields:

$$\langle xg(x) \rangle = \int_{-A}^{A} x^2 p(x) + 2A \int_A^\infty xp(x)\, dx = \sigma_x^2 \int_{-A}^{A} p(x)\, dx. \tag{A6}$$

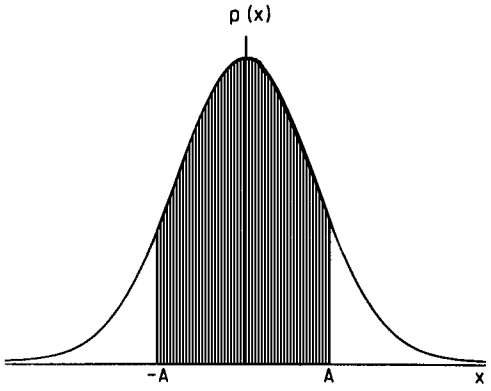


FIGURE 14. A Gaussian function (PDF) with the clipping or saturation levels set at $-A$ and $A$.

and the input-output cross-correlation gives:

$$K_1(f) = \frac{Y(f)X^*(f)}{\sigma_x^2} = \frac{Y(f)H^*(f)U^*(f)}{\sigma_x^2}. \tag{A7}$$

Then it follows that the resultant first-order Wiener kernel, $H_1(f)$, for this saturated linear system is:

$$H_1(f) = \frac{Y(f)U^*(f)}{\sigma_u^2} = H(f) \int_{-A}^{A} p(x)\, dx, \tag{A8}$$

with $H(f)$ being the transfer function of the linear subsystem.

Therefore, the gain factor is equal to the probability of the Gaussian $\int_{-A}^{A} p(x)\, dx > 0$ variable $x(t)$ within a range from $-A$ to $A$ (the shaded area in Fig. 14, which shows the levels of clipping). Such a factor is static and decreases as the modulation depth $\sigma_x$ becomes larger. Hence, the amplitude of the resultant Wiener kernel will be inversely proportional to the modulation depth and will have the same

phases and waveform as the original kernel. Here we note that Gaussian white noise is a modulation around a zero mean. In the case of light input, Gaussian modulation is around a mean luminance, $I_0$, and in the case of neuronal response the modulation is around a mean level of polarization, $V_0$.

This paper was edited by Hildred Machuca.

The research was supported by grants from the National Eye Institute, NEI08848 and NEI07738, and from the National Istitute of Neurological Diseases and Stroke, NS30772. K.-I. Naka is a Jules and Doris Stein Professor of Research to Prevent Blindness, Inc.

*Original version received 16 November 1994 and accepted version received 13 March 1995.*

## REFERENCES

Benardete, E. A., E. Kaplan, and B. W. Knight. 1992. Contrast gain control in the primate retina: P cells are not X-like, some M cells are. *Visual Neuroscience.* 8:483–486.

Bendat, J. S. 1990. Nonlinear System Analysis and Identification from Random Data. John Wiley & Sons, Inc., New York. 267 pp.

Chappell, R. L., K.-I. Naka, and M. Sakuranaga. 1985. Dynamics of turtle horizontal cell response. *Journal of General Physiology.* 86:423–453.

de Boer, E., and P. Kuyper. 1968. Triggered correlation. *IEEE Transactions in Biomedical Engineering.* 15:169–179.

Kaneko, A. 1970. Physiological and morphological identification of horizontal, bipolar, and amacrine cells in goldfish retina. *Journal of Physiology.* 207:623–633.

Korenberg, M. J. 1973. Identification of biological cascades of linear and static nonlinear systems. *Proceeding of 16th Midwestern Symposium on Circuit and Theory.* 18:1–9.

Korenberg, M. J., H. M. Sakai, and K.-I. Naka. 1989. Dissection of the neuron network in the catfish inner retina. III. Interpretation of spike kernels. *Journal of Neurophysiology.* 61:1110–1120.

Lawton, T. B., and C. W. Tyler. 1994. On the role of X and simple cells in human contrast processing. *Vision Research.* 34:659–667.

McKean, H. P. 1973. Wiener's theory of nonlinear noise. *In* Stochastic Differential Equations Proceedings of Society of Industrial and Applied Mathematics-American Mathematical Society. Vol. 6. J. S. Keller and H. P. McKean, editors. 191–209.

Meister, M., J. Pine, and D. A. Baylor. 1993. Multi-neuronal signals from the retina: Acquisition and analysis. *Journal of Neuroscience Methods.* 51:95–106.

Mizunami, M., H. Tateda, and K.-I. Naka. 1986. Dynamics of cockroach neurons. *Journal of General Physiology.* 88:275–292.

Naka, K.-I., and W. A. H. Rushton. 1966. S-potentials from luminosity units in the retina of fish (Cyprinidae). *Journal of Physiology.* 185:587–500.

Naka, K.-I., R. L. Chappell, M. Sakuranaga, and H. Ripps. 1988. Dynamics of skate horizontal cells. *Journal of General Physiology.* 92:811–831.

Naka, K.-I., R. Y. Chan, and S. Yasui. 1979. Adaptation in catfish retina. *Journal of Neurophysiology.* 42:441–454.

Naka, K.-I., M. A. Itoh, and R. L. Chappell. 1987. Dynamics of turtle cones. *Journal of General Physiology.* 89:321–337.

Naka, K.-I., and T. Ohtsuka. 1975. Morphological and functional identifications of catfish retinal neurons. II. Morphological identification. *Journal of Neurophysiology.* 38:72–91.

Naka, K.-I., and H. M. Sakai. 1991. Network mechanisms in the vertebrate retina. *News in Physiological Sciences.* 6:214–219.

Ohzawa, I., and R. D. Freeman. 1985. Contrast gain control in the cat visual system. *Journal of Neurophysiology.* 54:651–665.

Rushton, W. A. H. 1965. The Ferrier lecture: visual adaptation. *Proceedings of the Royal Society of London B.* 162:20–46.

Sakai, H. M., and K.-I. Naka. 1987*a*. Signal transmission in the catfish retina. IV. Transmission to ganglion cells. *Journal of Neurophysiology.* 58:1307–1328.

Sakai, H. M., and K.-I. Naka. 1987*b*. Signal transmission in the catfish retina. V. Sensitivity and circuit. *Journal of Neurophysiology.* 58:1329–1350.

Sakai, H. M., and K.-I. Naka. 1988. Neuron network in catfish retina: 1968–1987. *Progress in Retinal Research.* 7:149–208.

Sakai, H. M., and K.-I. Naka. 1992. Response dynamics and receptive-field organization of catfish amacrine cells. *Journal of Neurophysiology.* 67:430–442.

Sakuranaga, M., and Y.-I. Ando. 1985. Visual sensitivity and Wiener kernels. *Vision Research.* 25:507–510.

Sakuranaga, M., Y.-I. Ando, and K.-I. Naka. 1987. Dynamics of the ganglion cell response in the catfish and frog retina. *Journal of General Physiology.* 90:229–259.

Sakuranaga, M., and K.-I. Naka. 1985. Signal transmission in the catfish retina. II. Transmission to type-N cell. *Journal of Neurophysiology.* 53:390–410.

Shapley, R. M., and J. D. Victor. 1978. The effect of contrast on the transfer properties of cat retinal ganglion cells. *Journal of Physiology.* 285:275–298.

Shapley, R. M., and J. D. Victor. 1979. The contrast gain control of the cat retina. *Vision Research.* 19:431–434.

Shapley, R. M., and J. D. Victor. 1980. The effect of contrast on the nonlinear response of the Y cells. *Journal of Physiology.* 302:535–547.

Shapley, R. M., and J. D. Victor. 1981. How the contrast gain control modifies the frequency responses of cat retinal ganglion cells. *Journal of Physiology.* 318:161–179.

Shapley, R., and C. Enroth-Cugell. 1984. Visual adaptation and retinal gain control. *Progress in Retinal Research.* 4:263–346.

Shapley, R., E. Kaplan, and K. Purpura. 1993. Contrast sensitivity and light adaptation in photoreceptor or in the retinal network. *In* Contrast Sensitivity. R. Shapley and D. M.-K. Lam, editors. MIT Press, Cambridge, MA. 103–116.

Victor, J. D. 1987. The dynamics of the cat retinal X cell centre. *Journal of Physiology.* 386:219–246.

Victor, J. D. 1988. The dynamics of the cat retinal Y cell subunit. *Journal of Physiology.* 405:289–320.

Winslow, R. L., and S. Ma. 1990. Bifurcation analysis of nonlinear retinal horizontal cell models. II. Network properties. *Journal of Neurophysiology.* 64:248–261.